

## OPTIMIZING THE GAS FLOW THROUGH THE BREATHING APPARATUS MECHANISMS OF DIVERS WITH COMPUTATIONAL FLUID DYNAMICS

Tamara STANCIU<sup>1</sup>,  
Andrei SCUPI<sup>2</sup>, Cătălin FRĂȚILĂ<sup>3</sup>

**Rezumat:** Am verificat variația debitului volumic al gazului în trei variante constructive ale mecanismului de intrare a gazului regulatorului de presiune treapta a doua prin Computational Fluid Dynamics. Am făcut modelarea geometrică a celor trei variante. După discretizarea modelelor de fluid obținute, s-au stabilit condițiile de curgere necesare. S-au calculat debitul masic, densitatea gazului, la ieșirea mecanismului de reducere a presiunii și vitezele de fluid. Pentru aceleași condiții de curgere și aceeași depresiune de inhalare, am determinat rezistențele externe în trei variante geometrice ale mecanismului de admisie a gazului. Se poate concluziona că cea mai bună formă a orificiilor de admisie ale furtunului de presiune medie în regulatorul treapta a doua este cea cu secțiunea de cerc. Pentru piston, portul de direcție a fluxului de aer recomandat este secțiunea conică. Pentru a optimiza curgerea gazului prin restrictor, în proiectarea aparatului respirator, recomandăm ca geometria mecanismului de admisie să fie în varianta 1, cu 6 fante cilindrice, dar gaura din corpul pistonului să fie conică, ca în varianta 2. Folosind Computational Fluid Dynamics putem executa alte simulări cu caracteristici geometrice diferite până când obținem o formă optimă.

**Abstract:** We checked the variation of the gas volume flow in three design versions of the gas inlet in intake mechanism of the second stage pressure regulator by Computational Fluid Dynamics. We made the geometric modeling of three versions. After the meshing of the obtained fluid models, the required flow conditions were set. The mass flow rate, the gas density at the outlet of the pressure reducing mechanism and the fluid velocities were calculated. For the same flowing conditions and the same inhalation depression, we determined the external resistances in three chosen geometric versions of the gas intake mechanism. It can be concluded that the best shape of the inlets in the intake seat in second stage regulator is that of 2<sup>nd</sup> Version with conical section into the piston. To optimize gas flow through the restrictor, in the design of the breathing apparatus, we recommend that the inlet mechanism geometry be in 1<sup>st</sup> Version and 2<sup>nd</sup> Version, with 6 cylindrical slots, but the hole in the piston body to be conical, as in 2<sup>nd</sup> Version. Using Computational Fluid Dynamics we can run other simulations with different geometrical characteristics until we obtain an optimal shape.

**Keywords:** breathing apparatus, mechanism, gas flow, Computational Fluid Dynamics

---

<sup>1</sup>Ph.D student, Eng., Senior Researcher, "Diving Center", Constanta, Romania ([tamara.stanciu@navy.ro](mailto:tamara.stanciu@navy.ro))

<sup>2</sup>PhD, Lecturer, eng., "Maritime University", Constanta, Romania, ([andrei.scupi@gmail.com](mailto:andrei.scupi@gmail.com)).

<sup>3</sup>Junior Researcher, Eng., Had of Researcher Laboratory, "Diving Center", Constanta, Romania

---

## 1. Introduction

Breathing in the underwater environment is influenced by the increase in environmental pressure, where the respiratory gas is supplied by the diver's breathing apparatus. The gas becomes denser and the flow resistance increases when passing through the pressure reducer mechanism. The solution of avoiding adverse effects caused by increasing breathing resistance in the underwater environment is to obtain the optimal geometric shape of the pressure reducer mechanism.

The purpose of the paper is to identify, by simulating the flow of the respiratory mixture with Computational Fluid Dynamics, the geometric shapes of the gas inlet mechanisms that reduce the respiratory resistance.

## 2. Mechanisms of breathing apparatus

A second stage pressure regulator as schematically represented in Figure 1 takes up the intermediate pressure from the first stage and reduces it to ambient pressure, at which the diver can breathe without causing a physiological incident. When the diver inhales, the pressure inside the second stage decreases, causing a diaphragm to depress and actuate a lever. This lever opens the valve allowing air to come into the second stage and to the diver. When the diver exhales, the diaphragm is extended and the exhaled gas leaves the second stage through exhaust ports located at the bottom of the second stage. The pressure needed to move the lever into the open position is called the cracking pressure. The lower the cracking pressure the less breathing resistance is felt by the diver.

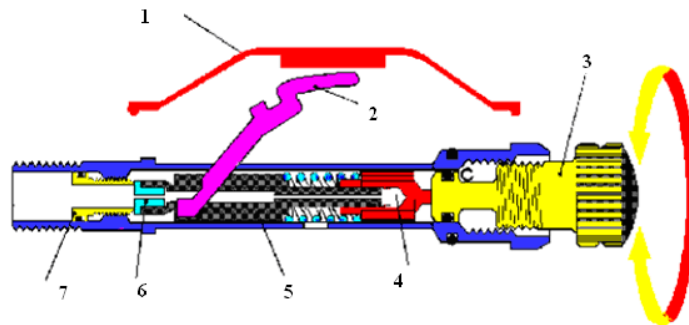


**Fig. 1. Operating of a second stage regulator with cracking resistance control [1].**

1. Diaphragm. 2. Lever. 3. Cracking resistance control. 4. Counter balance cylinder.

5. Poppet valve. 6. Rubber seating. 7. Seat.

Regulators are tested in USA using the National Agency for Science, Technology and Innovation (ANTSI) testing system. [2] This system evaluates regulators on human breathing simulation, scientific repeatability, test time, and complexity. Regulators are tested at several different breathing rates thus testing the regulator

at different tidal volumes as well. The different breathing rates and volume are referred to as the RMV or respiratory minute volume. This RMV is measured in liters per minute. The amount of energy expended by a diver is measured in joules per liter, for 1 litre of respiratory air, known as the work of breathing or WOB. Each manufacturer will test a regulator at their own chosen RMV. The results are generally compared to the goal set by the US Navy. The Navy prefers regulators that perform with a work of breathing at 1.3 [J/l] or less when breathed at 62.5 [l/min] RMV at 40 – 60 [mH<sub>2</sub>O] using a 10.3 • 10<sup>6</sup>[Pa] supply pressure.

We chose to study an unbalanced regulator Super Physalie, whose intake mechanism is represented in Figure 2. The studied pneumatic circuit has two points of interest: the variable restrictor 1 due to the x-displacement of the cylinder and the fixed restrictor 2, the hole in the cylinder. Flowing through the two restrictors at this moment is done with critical flow. The pressure is reduced by restrictors to the value of the outside pressure. In Restrictor 1, which is a Laval nozzle, the flow is turbulent for a short time and then becomes stationary.

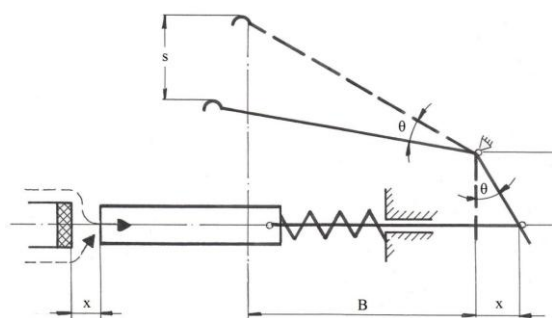


**Fig. 2.** Intake mechanism of the second stage regulator Super Physalie [3].

$x$  – displacement of the cylinder  
 $b, B$  - from the lever geometry  
 $s$  – lever displacement

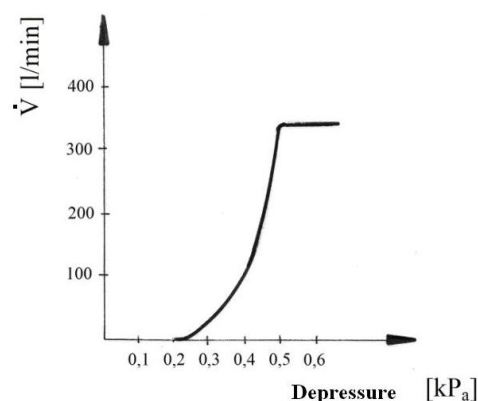


**Fig. 3.** Functional characteristic of the regulator in normobaric pressure [3].

The motion law of the mechanism which reduces the pressure is:

$$x = \frac{b}{B} s \quad (1)$$

The functional feature of a breathing apparatus is the volume flow curve - the inhale depression. Each respirator is accompanied by the delivery of this characteristic, determined in terms of normobaric pressure. The theoretical curve has a profile similar to that in Fig. 3. As we can see the increase of the inhaled

depression, the volumetric flow also increases, which when reaching a maximum value is blocked at this value under the conditions of constant normobaric pressure. Deviations of this curve from its original shape also implicitly influence breathing resistance of the device. The functional feature changes under hyperbaric conditions. At the same inhaled depression value, the same device delivers respiratory gas at a volumetric flow different from the surface and depending on the environmental pressure (dive depth).

As the absolute pressure of the medium increases, the density of the breathing gas increases and there is pressure loss on the circuit, losses which increase the external resistance and decrease the volume flow delivered by the apparatus to the same inhaled depression.

Breathing apparatus have in their geometry variable section restrictors classified into two large groups:

- a. downstream opening (the gas flow direction and the section increasing are same), such as Super Physalie;
- b. upstream opening (the direction of gas flow is opposite to the section increasing).

This variable section restrictor is a convergent-divergent nozzle (Laval), whose role is to reduce the pressure of the feed gas. When passing through the minimum section, gas reaches critical speed and pressure drops. Due to this difference between the critical pressure and the outlet pressure, an expanding gas jet with variable pressure is formed through a wave system.

It is useful to study the flow through the Laval nozzle. The minimum section, at which critical speed is reached, is the critical section and all the parameters involved are critical:

$V = a = c$ , the speed of sound under critical conditions,  $\rho_c, p_c, T_c$ . [3]. In the critical section, the maximum mass flow rate is reached and according to the continuity equation for a current tube in the permanent movement of a compressible fluid, the mass flow will be constant in any section of the tube.

$$\dot{m}_c = \rho_c \sigma_c c = \dot{m}_0 = \dot{m} \quad (2)$$

The distribution of speeds and pressures through the Laval nozzle is very well presented in Fig. 4. At pressure regulators, the variable restrictor is an orifice whose geometry causes the pressure drop and, implicitly, breathing resistance. The external resistance to breathing that most influences the flow through the second stage respirator is resistance to inhale. The simplest formula for determining external inspire resistance is the one obtained by dividing the inspire depression  $\Delta p_E$  into volume flow  $\dot{V}$ .

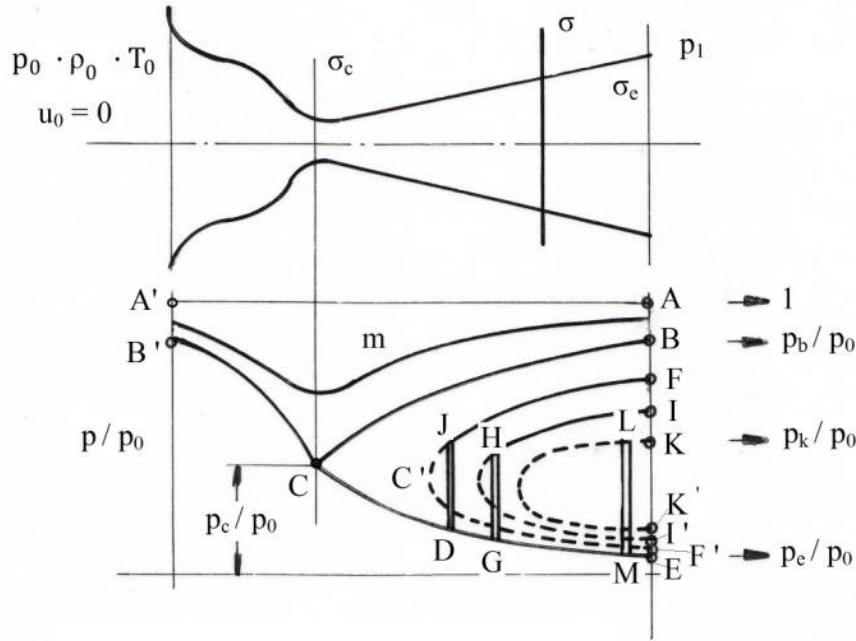


Fig. 4. Pressure distribution through the Laval nozzle [4].

$R_E = \Delta p_E / \dot{V}$	(3)
------------------------------	-----

The external resistance to breathing, induced by the second stage of regulator, at the gas flow is influenced by the geometric factors of the device:

- Inner diameters,
- The shape of the intake ports,
- Law of movement of intake mechanisms.

Our study refers to the influence of the geometric shape of the intake ports of the breathing apparatus by simulating the flow of the respiratory mixture with Computational Fluid Dynamics. [5].

### 3. The constructive versions chosen for the study

Flow variations in several scenarios for changing the inlet of the gas intake mechanism can be determined by simulating potential flow through the ANSYS Fluent program. The holes can be modified both dimensionally and in shape.

**1<sup>st</sup> Version** is the original downstream mechanism of the second stage regulator, with a six-hole seat in the same circle (see Fig. 5) and a cylindrical hole into piston (Fig. 6).

**2<sup>nd</sup> Version:** The hole in the piston is conical (Fig. 7.).



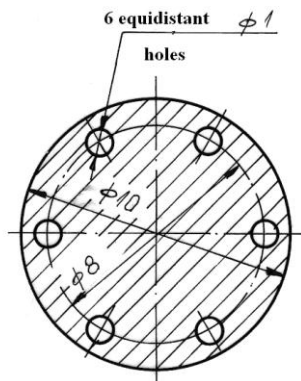
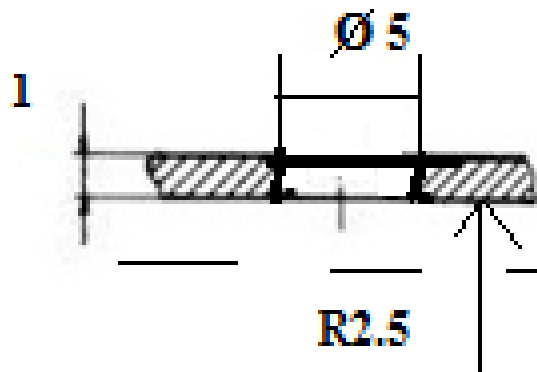
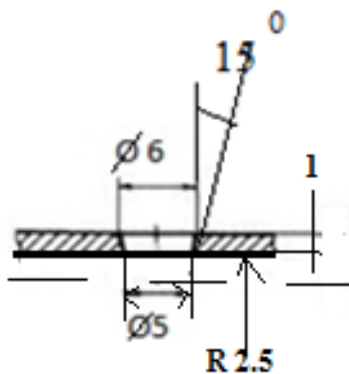
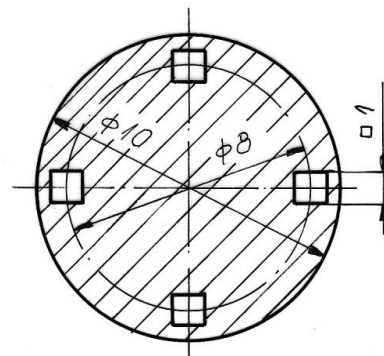


Fig. 5. Intake seat section.

Fig. 6. Cylindrical hole 1<sup>st</sup> Version.Fig. 7. Conical hole 2<sup>nd</sup> Version.Fig. 8. Modified seat section, 3<sup>rd</sup> Version.

**3<sup>rd</sup> Version:** I replaced the six intake of the seat with four other equidistant ones, placed on the same circle, but with the square section 1x1 (Fig. 8).

#### 4. Numerical simulation

We used all 5 parts of the ANSYS Fluent program [6], namely: Geometry, Meshing, Setting, Solution and Results, to determine the geometric conditions favorable to the reduction of external respiratory resistances. [5]

We modeled each of the three variants of the mechanism, starting from the original model: **1<sup>st</sup> Version, 2<sup>nd</sup> Version, and 3<sup>rd</sup> Version.**

After the modifications made, we separated the three mechanisms: **1<sup>st</sup> Version, 2<sup>nd</sup> Version, and 3<sup>rd</sup> Version.** (See Fig. 10. and Figure 11.).

Using operations specific to ANSYS Fluent, we simulated a cylindrical air stream to embrace these mechanisms and then remove them from the mechanisms (the Subtract command).

In this way we obtained the geometry of the fluid whose pressure is reduced in the three variants. (See Fig. 12.)





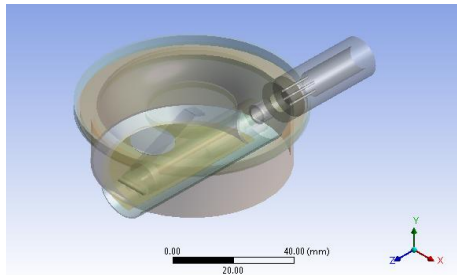


**Fig. 9.** Low pressure chamber of second stage.

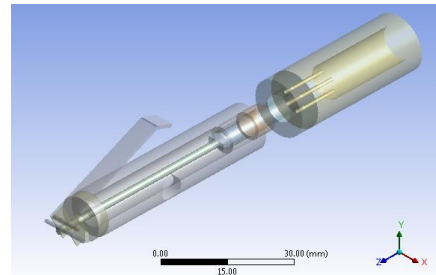


**Fig. 10.** 1<sup>st</sup> Version of pneumatic mechanism with cylindrical hole.

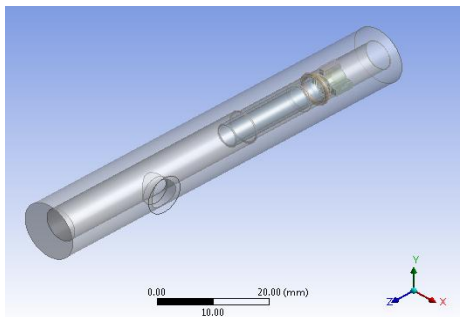


**Fig. 11.** 2<sup>nd</sup> Version of pneumatic mechanism with conical hole.

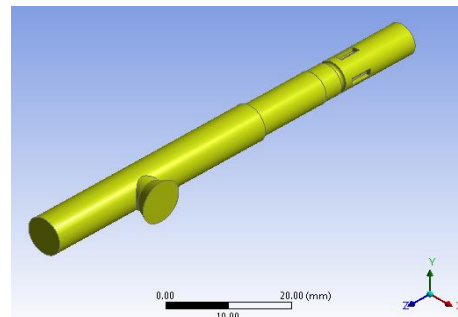


**Fig. 12.** 3<sup>rd</sup> Version Geometry of the air..

We went to step two, Meshing (see Fig. 13.) and we have established flow conditions (Setting):

1. Opening the piston  $x=0.7$  [mm],
2. Inhale depression  $\Delta p = 5$ [cmH<sub>2</sub>O],
3. Input pressure imposed  $p_i = 9$ [bar],
4. Output pressure  $p_e = 1$ [bar],
5. Respiratory gas: compressed air.

The finer the mesh used the better the results are. Convergence of Solutions is good (see Fig. 14) and we obtained the Results.

The results obtained were highlighted with the last part of the program, in the sections of interest, input and output, but also in planes parallel to the original coordinate axes.

By simulating with the ANSYS Fluent software, we have suggestively showed the pressure, speed and density distributions in the sections of interest of the chosen constructive versions. 1<sup>st</sup> Version (See Fig. 15), the inlet pressure through the critical section passes from the range  $9 \cdot 10^5$  Pa, after the restrictor to  $1.5 \cdot 10^5$  Pa and a return to  $4 \cdot 10^6$  Pa. At the piston outlet the pressure is  $1.5 \cdot 10^5$  Pa.



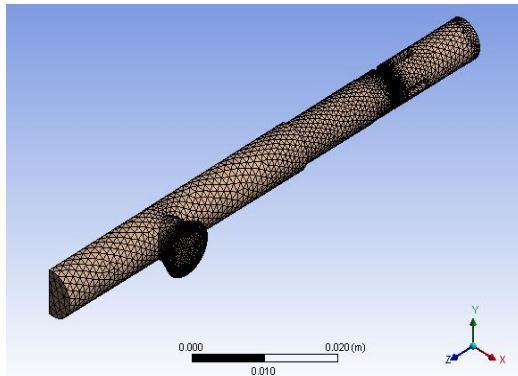


Fig. 13. 2<sup>nd</sup> Version Meshing.

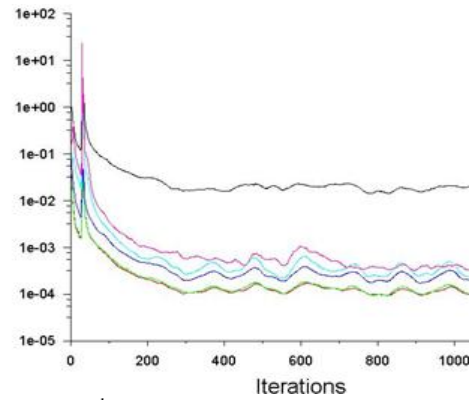


Fig. 14. 2<sup>nd</sup> Version Convergence of solutions.

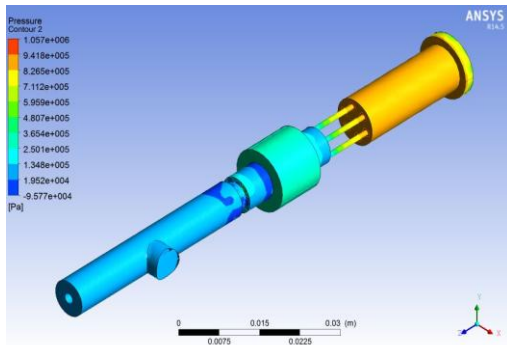


Fig. 15. 1<sup>st</sup> Version Distributions of pressures.

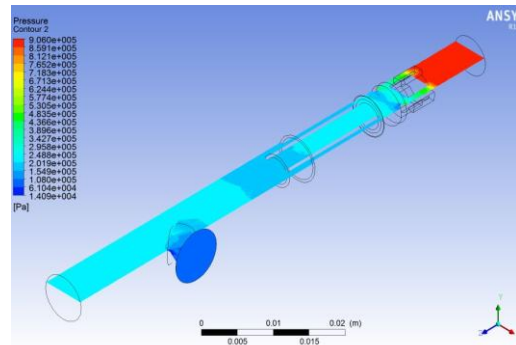


Fig. 16. 2<sup>nd</sup> Version Distributions of pressure.

2<sup>nd</sup> Version (See Fig. 16), the inlet pressure through the critical section passes from the range  $9 \cdot 10^5$  Pa, after the restrictor to  $3 \cdot 10^5$  Pa.

There is a marked drop in pressure on the plunger contour after the area of the O-ring,  $10^5$  Pa and then a slight return to  $2.5 \cdot 10^5$  Pa. The pressure is  $10^5$  Pa at the outlet through the conical opening.

In 1<sup>st</sup> Version (See Fig. 17) the speeds have a similar evolution, from 300 m / s at the entrance, to about 100 m / s at the exit. But when passing through the restrictor, a transient pass is made to the supersonic regime, specific to the Laval nozzle. For 3<sup>rd</sup> Version, the track of the gears is shown in Fig. 18. The velocity values are supersonic to the restrictor and subsonic (200-100 m/s) on the output contour. Using operations specific to ANSYS Fluent, we simulated a cylindrical air stream to embrace these mechanisms and then remove them from the mechanisms (the Subtract command). In this way we obtained the geometry of the fluid whose pressure is reduced in the three variants. (See Fig. 12).

Evolution of densities for 2<sup>nd</sup> Version is shown in Fig. 19: between 9 [kg/m<sup>3</sup>] at input and 2.11 [kg/m<sup>3</sup>] at the outlet.



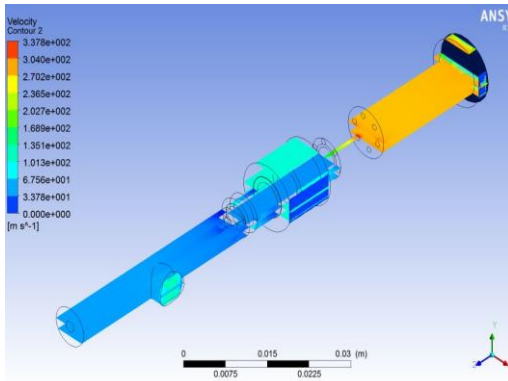


**Fig. 17.** 1<sup>st</sup> Version Distributions of air speed

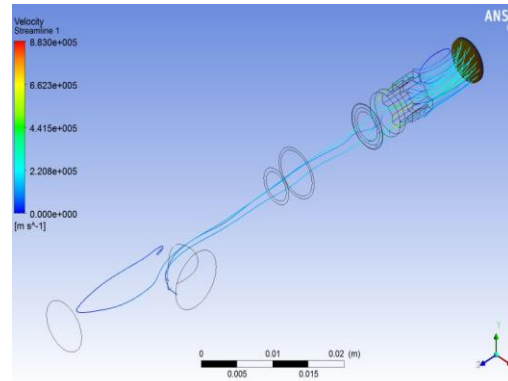


**Fig. 18.** 3<sup>rd</sup> Version Speed lines.

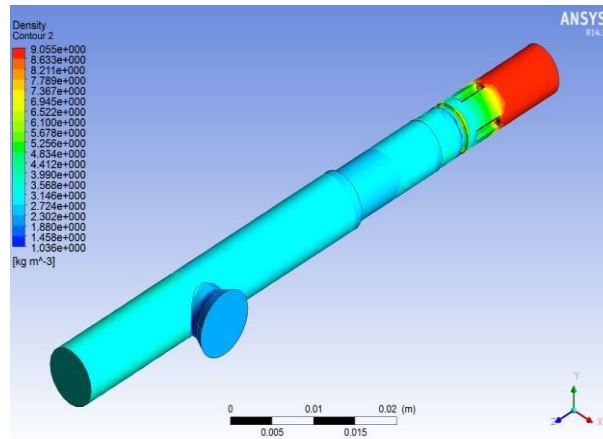


**Fig. 19.** 2<sup>nd</sup> Version Distributions of densities.

The mass flow is constant for the same flow conditions at the same apparatus. It depends on the opening of the restrictor (in this case we set  $x = 0.7$  mm constant for all three constructive versions chosen). Mass flows and the results obtained by numerical simulation, with the three geometric versions, chosen for the pressure regulator, are shown in Table 1.

Using operations specific to ANSYS Fluent, we simulated a cylindrical air stream to embrace these mechanisms and then remove them from the mechanisms (the Subtract command).

In this way we obtained the geometry of the fluid whose pressure is reduced in the three variants (See Fig. 12). Knowing the mass flow, we calculated the volume flow. For each case, we calculated the external resistance at the piston outlet, with formula (3).

$$\dot{V} = Q_m / \rho [l / \text{min}] \quad (4)$$

**Table 1.** The theoretical results obtained by numerical simulation

Model of the mechanism	$Q_m \left[ \frac{kg}{s} \right]$	$\rho [kg/m^3]$ exit of the cylinder	$\dot{V} [l/s]$ fixed restrictor	$\Delta p = 5 [cmH_2O]$	$R_E \left[ \frac{cmH_2O}{l/s} \right]$
1 <sup>st</sup> Version	$15,225 \cdot 10^{-3}$	2,842	5,357	5	0,933
2 <sup>nd</sup> Version	$13,433 \cdot 10^{-3}$	2,118	6,342	5	0,788
3 <sup>rd</sup> Version	$14,445 \cdot 10^{-3}$	3,724	3.879	5	1,289

## 5. Conclusions

Table 1 compares the results obtained for external inspiration resistance by simulating the air flow through the three geometric variants of the pressure regulator intake mechanism under the same conditions.

Observing the results obtained in Figures 15-19 and Table 1, one can conclude:

- The best shape of the holes in the intake seat is 6-point, equidistant, small diameter ( $\phi = 1mm$ )
- For the piston, the recommended airflow port is the conical one.

To optimize gas flow through the restrictor, in the design of the respirator, it is recommended that the geometry of the mechanism be with the 6 cylindrical slots on the intake seat and the hole in the piston body be conical, as in 2<sup>nd</sup> Version. The results obtained from the theoretical calculations and numerical simulation (Computational Fluid Dynamics) were experimentally tested on a professional test bench for two design versions of the gas direction port in the cylindrical pressure reducer piston (1<sup>st</sup> Version and 2<sup>nd</sup> Version).

## REFERENCES

- [1] Myers J., Clauson J, "*The design of Scuba Diving Regulators and Breathing Resistance*", (California University, **2006**.)
- [2] Bailey N, Bolsover J, Parker C & Hughes A, "*Performance of diving equipment*", HSE BOOKS, **2006**.
- [3] Constantin A., „*Transportul gazelor prin sistemul respirator uman și mijloacele de protecție a respirației, în procesele hiperbare*“, Ovidius University Press, Constanța, **2003**, pag. 72, 76.
- [4] Carafoli E., „*Dinamica fluidelor compresibile*“, Editura Academiei R.S.R., București **1984**, pag. 127, 130.
- [5] Scupi A, Dinu D., "*Fluid Mechanics Numerical Approach*", Ed. Nautica, Constanța, **2015**.
- [6] \*\*\*ANSYS Fluent Users Guide, **2012**, [www.pdfdrive.net/ansys-fluent-users-guide](http://www.pdfdrive.net/ansys-fluent-users-guide).
-